Nuclear Materials and Energy 43 (2025) 101929

Contents lists available at ScienceDirect

Nuclear Materials and Energy

journal homepage: www.elsevier.com/locate/nme

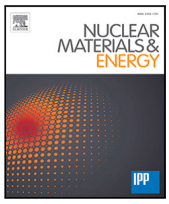

Impact of nitrogen molecular breakup on divertor conditions in JET L-mode plasmas using SOLPS-ITER

R. Mäenpää [a,*], H. Kumpulainen [a], M. Groth [a], N. Horsten [b], D. Reiter [c], J. Romazanov [d], B. Lomanowski [e], S. Brezinsek [d], J. Karhunen [f], K.D. Lawson [g], A.G. Meigs [g], S. Menmuir [g], A. Shaw [g], JET Contributors[1], EUROfusion Tokamak Exploitation Team[2]

[a] Aalto University, Espoo, Finland
[b] KU Leuven, Leuven, Belgium
[c] Institute for Laser and Plasma Physics, Heinrich-Heine-University, Düsseldorf, Germany
[d] Forschungszentrum Jülich GmbH, Jülich, Germany
[e] Oak Ridge National Laboratory, Oak Ridge, TN, USA
[f] VTT Technical Research Centre of Finland, Espoo, Finland
[g] UKAEA, Abingdon, United Kingdom

ARTICLE INFO

Keywords:
Nitrogen
Molecule
Recycling
JET
Divertor
SOLPS-ITER
L-mode

ABSTRACT

SOLPS-ITER simulations of nitrogen-seeded, low-confinement mode plasmas in the Joint European Torus (JET) predict that the electron temperature in the low-field side (LFS) divertor leg is reduced locally by up to an order of magnitude when nitrogen is assumed to recycle as molecules (N_2) instead of atoms using a fixed nitrogen injection rate. The LFS divertor temperature reduction under the assumption of molecular recycling occurs due to a three-step mechanism: (1) the plasma penetration of nitrogen atoms is increased due to the strong triple bond of the N_2 molecule and the kinetic energy release in the dissociation event, both mechanisms contributing equally, (2) the abundance of (particularly multiply-charged) nitrogen ions in the divertor is increased and (3) the electron temperature is reduced due to the increase in radiation (by up to a factor of 4) from nitrogen ions.

Setting the volume-integrated nitrogen radiated power to a constant value (0.6 MW) instead of the nitrogen injection rate, SOLPS-ITER predicts under the molecular nitrogen recycling assumption that the peak line-integrated N II, N III and N IV intensities in the LFS divertor are approximately within 15%, 35% and 5%, respectively, of the reference atomic nitrogen recycling case. The predicted peak N II, N III and N IV intensities under either assumption are within 30%, 65% and 5%, respectively, of measurements using the vertically viewing mirror-link divertor spectrometer (Meigs et al., 2010) in nitrogen-seeded JET L-mode plasmas (Lomanowski et al., 2019). ERO2.0 simulations using a constant nitrogen seeding rate on static background plasma solutions from EDGE2D-EIRENE (previously presented in Mäenpää et al., (2022), revised here to include fast reflections) predict that N II to N IV line emission is increased by 20% to 30% when nitrogen is assumed to recycle as molecules, demonstrating the importance of considering the effect of molecular dissociation reactions on the divertor plasma in a self-consistent manner.

1. Introduction

Injection of nitrogen gas has been used in the ASDEX Upgrade and JET tokamaks to achieve simultaneous divertor detachment with suppressed edge-localised modes (ELMs) in high-confinement mode (H-mode) operation [1,2], demonstrating the potential of nitrogen gas injection to protect divertor targets from excessive heat loads. In this contribution, we employ SOLPS-ITER [3] simulations of nitrogen-seeded, partially detached low-confinement mode (L-mode) JET plasmas to study the impact of nitrogen molecular (N_2) recycling on the

* Correspondence to: Aalto University, Otakaari 1, 02150 Espoo, Finland
E-mail address: roni.maenpaa@aalto.fi (R. Mäenpää).

[1] See the author list of "Overview of T and D-T results in JET with ITER-like wall" by CF Maggi et al. to be published in Nuclear Fusion Special Issue: Overview and Summary Papers from the 29th Fusion Energy Conference (London, UK, 16-21 October 2023).

[2] See the author list of "Overview of the EUROfusion Tokamak Exploitation programme in support of ITER and DEMO" by E. Joffrin Nuclear Fusion 2024 10.1088/1741-4326/ad2be4.

https://doi.org/10.1016/j.nme.2025.101929
Received 4 July 2024; Received in revised form 28 February 2025; Accepted 29 March 2025
Available online 12 April 2025

divertor plasma conditions.

Previously, ERO2.0 [4] simulations on static background plasma solutions from EDGE2D-EIRENE [5,6] predicted that assuming molecular recycling of nitrogen increases the peak line-integrated *N* III and *N* IV intensities (spectroscopic notation for N^{2+} and N^{3+}, respectively) by up to a factor of two across the low-field side (LFS) divertor, and increases the time-averaged, volume-integrated number of N^{5+} to N^{7+} ions in the plasma by approximately a factor of two [7]. Using SOLPS-ITER, which allows nitrogen molecules to be included, we are able to self-consistently take in to account the impact of the increased radiation from and abundance of multiply-charged nitrogen ions on the divertor plasma solution. Additionally, we revise ERO2.0 simulations from [7] to include the fast reflection of nitrogen ions.

2. Nitrogen divertor spectroscopy in partially detached JET L-mode plasmas

Measurements by the vertically-viewing mirror-link divertor spectrometer [8] (JET diagnostic KT3A/B) in partially detached JET L-mode discharges (JET pulse numbers 90416-90423) are used for the code-experiment comparison in this work. In these discharges, the toroidal field was 2.5 T, the plasma current 2.5 MA and the ion $\mathbf{B} \times \nabla B$-drift pointed into the divertor. Neutral beam heating (1.8 MW) was employed in addition to Ohmic heating (1.6 MW). The low-field side strike point was situated on the nearly horizontal target plate (JET divertor tile 5, stack C), enabling the vertically-viewing divertor spectrometers to infer the approximate radial and poloidal position of the nitrogen radiation front across the low-field side divertor leg (Fig. 1 in [9]).

Nitrogen was injected as molecules into the low-field side scrape-off layer from a toroidally distributed gas injection module, situated radially approximately 10 cm outboard from the low-field side strike point (Fig. 1 in [9]). The line-integrated core plasma density was held fixed to produce high-recycling conditions at the onset of divertor detachment, and the nitrogen seeding rate was increased from pulse to pulse. The highest non-disrupting nitrogen injection rate (approximately 1.6×10^{21} N atomic equivalents per second) was achieved in pulses 90422 and 90423. For an in-depth characterisation of the spectroscopic setup in JET pulses 90422 and 90423, as well as time series of line-integrated density, nitrogen injection rate, heating power and radiated power, see Section 4.1 and Fig. 7, respectively, in [10].

3. Setup of SOLPS-ITER simulations

SOLPS-ITER simulations (see Table A.3 for a catalogue) are set up using the EDGE2D-EIRENE simulations in [7,9] as a reference. In [7], it was found that the location and shape of the nitrogen emission front predicted by EDGE2D-EIRENE in the low-field side divertor is highly sensitive to $n_{\mathrm{e,sep,LFS-mp}}$, the electron density at the low-field side midplane separatrix. In the simulations of this contribution, $n_{\mathrm{e,sep,LFS-mp}}$ is fixed to $1.8 \times 10^{19}\,\mathrm{m}^{-3}$ (held constant by feedback injection of D_2 from the private-flux region), yielding the best agreement between SOLPS-ITER and EDGE2D-EIRENE predictions and divertor spectrometer measurements of line-integrated *N* II, *N* III and *N* IV intensity, when the other input parameters of the simulations are fixed to those we describe below. In the experiment, $n_{\mathrm{e,sep,LFS-mp}}$ was estimated to be higher ($2.0 \times 10^{19}\,\mathrm{m}^{-3}$ to $2.2 \times 10^{19}\,\mathrm{m}^{-3}$, Fig. 2 in [9]) than the optimal value of $1.8 \times 10^{19}\,\mathrm{m}^{-3}$ found in this contribution, possibly due to the lack of cross-field drifts in the SOLPS-ITER and EDGE2D-EIRENE simulations and/or the uncertainty of the separatrix location in the EFIT [11] equilibrium reconstruction. The reduction of $n_{\mathrm{e,sep,LFS-mp}}$ from $2.0 \times 10^{19}\,\mathrm{m}^{-3}$ to $1.8 \times 10^{19}\,\mathrm{m}^{-3}$ increases the predicted electron temperature in the divertor locally by up to a factor of five and reduces the electron density locally by up to a factor of four.

The cross-field particle diffusivities of D^+ ($D_\perp$) and N^+ to N^{7+} ($D_{\perp,\mathrm{N}}$) are set to $D_\perp = D_{\perp,\mathrm{N}} = 1.0\,\mathrm{m}^2\,\mathrm{s}^{-1}$, with the exception of $D_\perp = 0.5\,\mathrm{m}^2\,\mathrm{s}^{-1}$ in the area extending 1 cm radially to either direction from the separatrix, including in the divertor volume. The particle pinch velocities for D^+ and N^+ to N^{7+} are set to zero. The electron and ion heat diffusivities are set to $\chi_e = \chi_i = 1.0\,\mathrm{m}^2\,\mathrm{s}^{-1}$ inside the separatrix, and to $\chi_e = \chi_i = 0.5\,\mathrm{m}^2\,\mathrm{s}^{-1}$ outside the separatrix. The power crossing the core boundary of the simulation domain ($\rho_N = 0.8$) is set to 3.2 MW, assuming that 200 kW is radiated inside the core boundary. The predicted electron temperature at the low-field side midplane separatrix is 62 eV, within the measured range of 60 eV to 70 eV (Fig. 2 in [9]). The main chamber wall is assumed to consist of pure beryllium, and the divertor targets to consist of pure tungsten. Neither beryllium nor tungsten is included as a plasma species in the simulations.

Nitrogen is injected as atoms in to the low-field side scrape-off layer from the same poloidal location as in the experiment (Fig. 1 in [9]). The injection of molecular nitrogen is not studied in this contribution, as its effect on the emission from and abundance of multiply-charged nitrogen ions in comparison to molecular recycling was previously shown to be negligible [7] due to the recycling source dominating over the injection source. The option to use feedback injection of impurities to fix the impurity radiated power was not available in SOLPS-ITER at the time of this study. Therefore, a nitrogen injection scan was conducted.

Nitrogen is assumed to be a fully recycling species, i.e., the fraction of nitrogen ions and atoms incident on a target that does not undergo fast reflection is assumed to thermally recycle. The kinetic energy of the thermally recycled nitrogen atoms (or nitrogen molecules, if molecular recycling is assumed) is set to a constant 0.074 eV, corresponding to an assumed wall temperature of 300 °C. Nitrogen molecules and molecular ions do not undergo fast reflection, and are instead assumed to thermally recycle. The fraction of fast reflections and the energy of the reflected nitrogen atoms is calculated using the TRIM-database [12]. Carbon-on-tungsten TRIM-data is substituted for nitrogen-on-tungsten data (as in EDGE2D-EIRENE due to limited input options), leading to an underestimation of the nitrogen radiated power by up to 5%.

A pump is included in the low-field side divertor corner with an albedo of 0.8 as determined for hydrogenic species in [13]. We assume the pump albedo to be 0.8 also for nitrogenic species (see Section 9 for discussion). The simulations in this work have reached a steady-state, where the nitrogen injection rate equals the pumping rate (with each pumped N_2 molecule counting as two atoms). The subdivertor volume is not included in these simulations due to the expected negligible impact on the low-field side divertor plasma conditions [14] (although the inclusion of the subdivertor volume may impact the pumping rate, see Section 9). In the simulations where the thermally-released fraction of nitrogen is assumed to recycle as molecules, a minimal set of electron impact reactions for molecular nitrogen from the AMJUEL database [15] is included (Table 1). The ray tracing code Cherab [16] is used for calculating line-integrated nitrogen ion emission intensities based on the predictions from SOLPS-ITER, taking into account the reflections from the metallic JET ITER-like wall.

4. Setup of EDGE2D-EIRENE and ERO2.0 simulations

EDGE2D-EIRENE simulations of nitrogen-seeded JET L-mode plasmas first setup in [9], and used for sensitivity studies and as background plasmas for ERO2.0 simulations in [7], are compared in this work to the SOLPS-ITER simulations and used as background plasmas for revised ERO2.0 simulations (with minor modifications to the input options). The settings in the SOLPS-ITER simulations of this work described in Section 3 are also used in the EDGE2D-EIRENE simulations with two exceptions. First, feedback injection of nitrogen is used in EDGE2D-EIRENE to set the nitrogen radiated power to 0.6 MW (based on bolometric estimates in [9]). The steady-state injection rate needed to reach $P_{\mathrm{rad,N}} = 0.6$ MW in EDGE2D-EIRENE is 6.1×10^{19} *N* atoms per second. Second, nitrogen molecules are not included in the EDGE2D-EIRENE simulations, as they were not available at the time of this study as an input option.

Table 1
AMJUEL reaction identifiers, reaction equations, electron energy loss and kinetic energy release values for the minimal set of nitrogen molecular electron impact reactions from [15]. The impacting electron has been omitted from the reaction equations for brevity. The rate coefficients of these reactions are of the single-parameter type, i.e. they depend only on the electron temperature and not on the electron density. *Reaction 2.7.14 (included only in the SOLPS-ITER simulations) has no threshold and its associated electron energy loss value is calculated from the electron energy weighted rate coefficient.

AMJUEL	Reaction	ΔE_{el} (eV)	KER (eV)
2.7.5	$N_2 \longrightarrow 2N$	9.75	0.95
2.7.9	$N_2 \longrightarrow e + N_2^+$	15.6	0.0
2.7.10	$N_2 \longrightarrow e + N + N^+$	24.3	8.0
2.7.11	$N_2^+ \longrightarrow e + 2N^+$	31.2	11.8
2.7.12	$N_2^+ \longrightarrow N + N^+$	8.4	1.0
2.7.14	$N_2^+ \longrightarrow 2N$	*	3.5

ERO2.0 simulations used in [7] to model nitrogen molecular recycling on static background plasmas from EDGE2D-EIRENE simulations are revised in this contribution to include the fast reflection of nitrogen ions and atoms (missing due to a software issue in the previous contribution). The nitrogen transport and surface interaction settings in the SOLPS-ITER simulations of this work described in Section 3 are also used in the ERO2.0 simulations. The nitrogen injection rate, however, is fixed to the steady-state rate in the EDGE2D-EIRENE simulations, i.e. 6.1×10^{19} N atoms per second. ERO2.0 includes the same set of nitrogen molecular dissociation reactions as the SOLPS-ITER simulations in this work (Table 1), with the exception that reaction 2.7.14 is only included in the SOLPS-ITER simulations. The EDGE2D-EIRENE and ERO2.0 simulations are both post-processed using Cherab to obtain line-integrated nitrogen ion intensities.

5. Impact of molecular recycling on divertor plasma conditions in SOLPS-ITER simulations

When nitrogen is assumed to recycle as N_2 molecules instead of N atoms, and the nitrogen injection rate is fixed to 3×10^{19} N atoms per second, SOLPS-ITER predicts that the electron temperature in the low-field side divertor leg is reduced locally by up to an order of magnitude (Fig. 1). Concomitantly, SOLPS-ITER predicts electron density to increase by up to a factor five when molecular recycling is assumed (figure omitted). The electron temperature reduction due to nitrogen recycling as N_2 occurs in a volume approximately coincident with the peak emission from N II to N IV (figure omitted). At the low-field side strike point the difference in electron temperature between the simulations is less than a factor of two due to detached conditions (electron temperature < 1 eV) already prevailing at the strike point in the molecular recycling simulation.

When the nitrogen injection rate is varied in the SOLPS-ITER simulations (Fig. 2), roll-over of the electron density and reduction of the electron temperature to below 1 eV at the low-field side strike point occur at a lower injection rate (3×10^{19} N atoms per second) when nitrogen is assumed to recycle as molecules than under the atomic recycling assumption (9×10^{19} N atoms per second). SOLPS-ITER also predicts that the power radiated by nitrogen ions ($P_{rad,N}$) increases faster as a function of the nitrogen injection rate when N_2 recycling of nitrogen is assumed (Fig. 3). The bolometric estimate of 0.6 MW of power radiated by nitrogen is reached at an injection rate of approximately 6×10^{19} and 2.1×10^{20} N atoms per second in the molecular and atomic nitrogen recycling simulations, respectively. The maximum power radiated by nitrogen at which a steady-state solution is obtained under the molecular recycling assumption is approximately 1.8 MW, and 0.65 MW when nitrogen is assumed to recycle as N atoms.

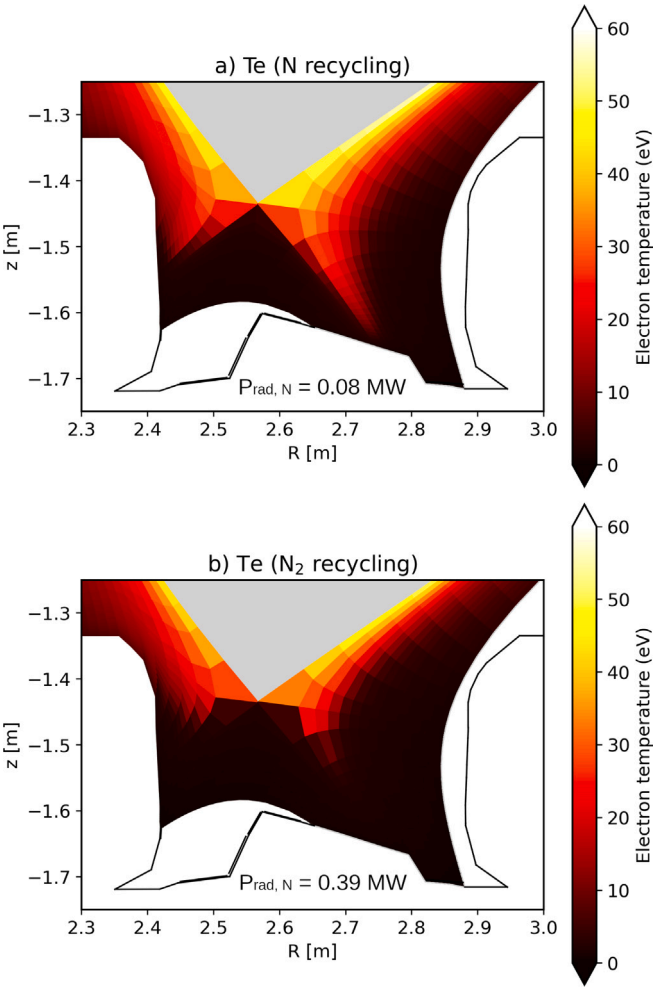

Fig. 1. Electron temperature in the divertor predicted by SOLPS-ITER under the assumption that (a) nitrogen recycles as N atoms and (b) nitrogen recycles as N_2 molecules. The nitrogen injection rate in simulations a and b is fixed to 3×10^{19} N atoms per second and the electron density at the low-field side midplane separatrix $n_{e,sep,LFS-mp}$ is fixed to 1.8×10^{19} m^{-3}.

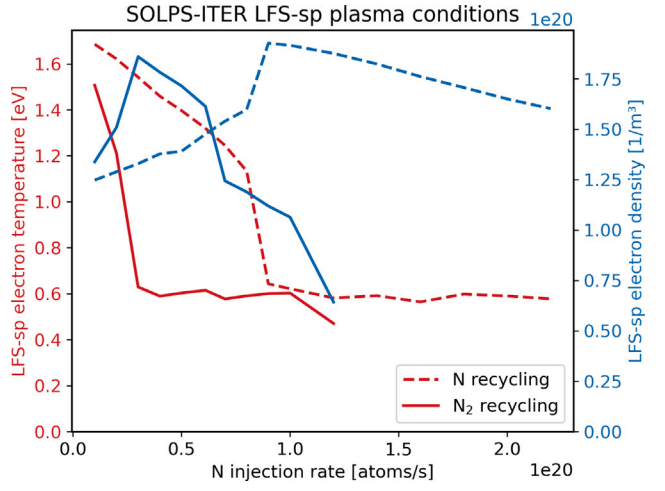

Fig. 2. Electron temperature and electron density at the low-field side strike point predicted by SOLPS-ITER versus the nitrogen injection rate under the assumptions that nitrogen recycles as N atoms (dashed lines) and that nitrogen recycles as N_2 molecules (solid lines). The electron density at the low-field side midplane separatrix $n_{e,sep,LFS-mp}$ has been fixed to 1.8×10^{19} m^{-3} in both simulations.

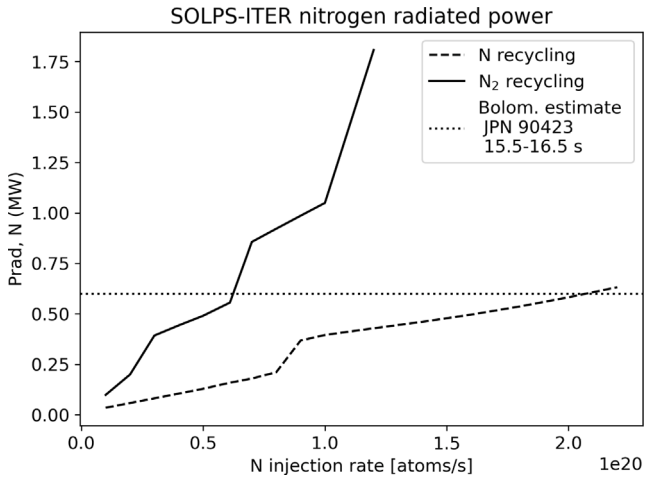

Fig. 3. SOLPS-ITER prediction of the (volume-integrated) power radiated by nitrogen ions versus the nitrogen injection rate under the assumptions that nitrogen recycles as N atoms (dashed line) and that nitrogen recycles as N_2 molecules (solid line). The horizontal line represents the bolometric estimate of power radiated by nitrogen in JPN 90423 between 15.5 s to 16.5 s. The electron density at the low-field side midplane separatrix $n_{e,sep,LFS-mp}$ has been fixed to $1.8 \times 10^{19}\,m^{-3}$ in both simulations.

6. Physical mechanism of temperature reduction in the low-field side divertor leg under the nitrogen molecular recycling assumption

The increase in nitrogen radiated power (Fig. 3) and the associated reduction in the nitrogen injection rate at which the low-field side strike point temperature is reduced below 1 eV and at which electron density roll-over occurs (Fig. 2) under the molecular recycling assumption is due to an increase in the abundance of nitrogen ions in the plasma. When nitrogen is assumed to recycle as N_2 molecules instead of N atoms, and the nitrogen injection rate fixed to 3×10^{19} N atoms per second, SOLPS-ITER predicts that the volume-integrated number of singly-charged nitrogen ions is increased by 80%, the number of doubly-charged nitrogen ions by a factor of 7 and the number of N^{3+} to N^{7+} ions by a factor of 3 to 4. We hypothesise that the increase in nitrogen ion abundance is due to enhanced plasma penetration of nitrogen atoms, which in turn increases the likelihood of N^+ ions to be ionised to higher charge states due to the longer mean dwell time in and better access to high temperature regions of the plasma.

SOLPS-ITER predicts that under the nitrogen molecular recycling assumption the ionisation source of N^+ ions is increased in magnitude to accommodate the increased abundance of multiply-charged nitrogen ions and moved towards the X-point from the target (Fig. 4), which is consistent with an increase in the plasma penetration of neutral nitrogen atoms and a reduction in the divertor temperature due to the increase in nitrogen radiated power. In a coupled SOLPS-ITER simulation the reduction in electron temperature (in the B2 plasma solution) and the increase in plasma penetration of neutral nitrogen molecules and atoms (as determined by EIRENE) occur in a step-wise manner over a large number of iterations when N_2 recycling is enabled. Thus, the movement of the ionisation front is a cumulative process, the result of which is shown in Fig. 4 b.

The increase in plasma penetration of nitrogen atoms under the molecular recycling assumption is attributed to two mechanisms. First, a nitrogen molecule is only dissociated by sufficiently energetic electrons. The N_2 dissociation threshold (9.75 eV) is high due to the triple bond of the N_2 molecule. Secondly, the dissociation fragments (N or N^+ depending on the reaction) gain translational energy (KER) in the dissociation event (Fig. 5). By decreasing the KER values of the molecular dissociation reactions in Table 1 by a factor of 1000 (chosen arbitrarily) so that the translational energy imparted on to the dissociation fragments is less than one fifth of the assumed thermal recycling energy (0.074 eV), SOLPS-ITER predicts that the power radiated by nitrogen ions is reduced from approximately 0.2 MW to 0.13 MW (Table 2). Additionally, increasing the rate coefficient of reaction 2.7.5

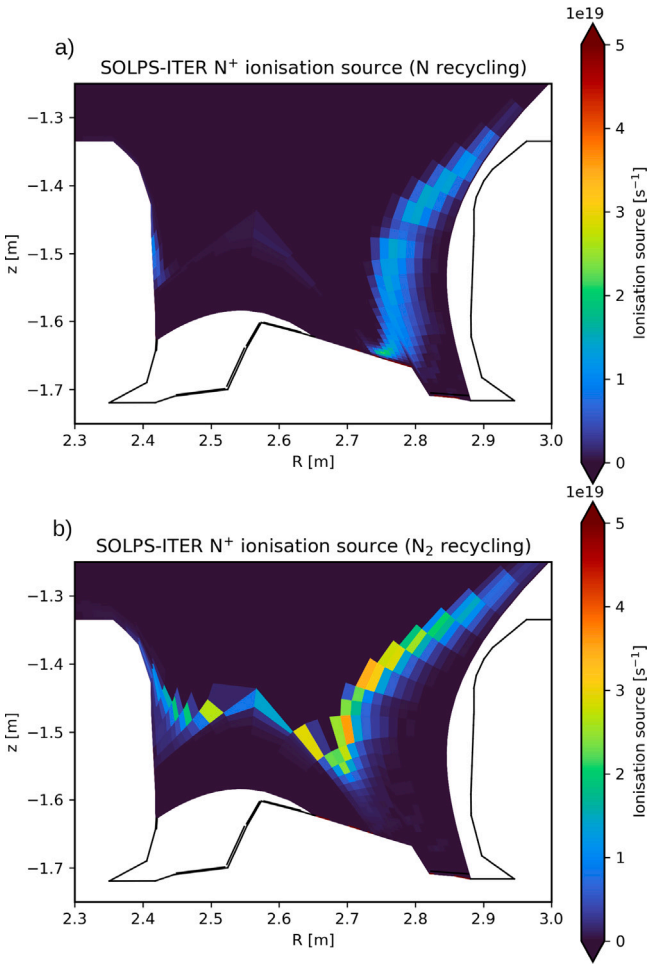

Fig. 4. Ionisation source of singly-charged nitrogen ions predicted by SOLPS-ITER assuming that (a) nitrogen recycles as atoms and (b) nitrogen recycles as molecules. The nitrogen injection rate in simulations a and b is fixed to 3×10^{19} N atoms per second and the electron density at the low-field side midplane separatrix $n_{e,sep,LFS-mp}$ is fixed to $1.8 \times 10^{19}\,m^{-3}$.

Table 2
Plasma parameters at the low-field side strike point and the volume-integrated nitrogen radiated power from five SOLPS-ITER simulations: (1) nitrogen recycles as N atoms (2) nitrogen recycles as N_2 molecules (3) nitrogen recycles as N_2 molecules, but the electron energy loss of dissociation and ionisation reactions in Table 1 is set to zero (4) nitrogen recycles as N_2 molecules, but the kinetic energy release values (KER) of reactions in Table 1 are divided by 10^3 (5) nitrogen recycles as N_2 molecules, the KER values of reactions in Table 1 are divided by 10^3 *and* the rate coefficient of AMJUEL reaction 2.7.5 ($e + N_2 \longrightarrow e + 2N$) is multiplied by 50. In all five simulations, the nitrogen injection rate is fixed to 2×10^{19} N atoms per second and the electron density at the low-field side midplane separatrix $n_{e,sep,LFS-mp}$ is fixed to $1.8 \times 10^{19}\,m^{-3}$.

Param.	N only	N_2 rec.	N_2 rec., $\Delta E_{el} = 0$ eV	N_2 rec., KER/10^3	N_2 rec., KER/10^3, $\langle \sigma v \rangle_{2.7.5} \cdot 50$
$T_{e,LFS-sp}$ (eV)	1.63	1.2	1.2	1.38	1.62
$n_{e,LFS-sp}$ ($10^{20}\,m^{-3}$)	1.62	1.85	1.86	1.76	1.62
$P_{rad,N}$ (kW)	58	199	199	127	57

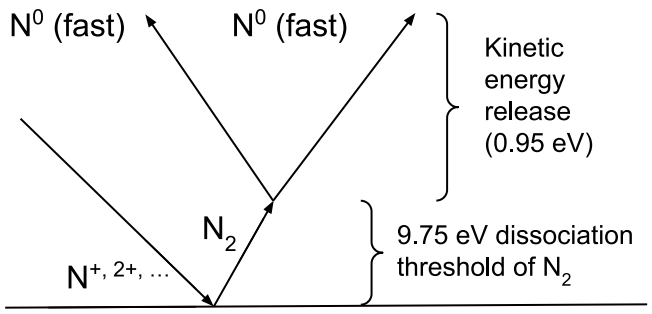

Fig. 5. Physical mechanism of increased plasma penetration of nitrogen atoms under the molecular recycling assumption: (1) a nitrogen molecule is released from the divertor target after thermalisation, and dissociates only upon impact by sufficiently energetic electrons (2) in the dissociation event, the dissociation fragments (here, *N* atoms) gain translational energy, travelling further into the plasma on average than a thermally recycled *N* atom would. AMJUEL reaction 2.7.5 ($e + N_2 \longrightarrow e + 2N$) is depicted, but other dissociation pathways are also possible Table 1.

(which produces two neutral nitrogen atoms) by a factor of 50 (chosen arbitrarily) and thus greatly reducing the lifetime of the N_2 molecules, SOLPS-ITER predicts that the power radiated by nitrogen ions is further reduced to the value predicted in the atomic recycling simulation (from 0.13 MW to 0.06 MW). Thus the kinetic energy release in the dissociation event and the high dissociation threshold of the N_2 molecule contribute approximately equally to the increase in the nitrogen radiated power under the nitrogen molecular recycling assumption.

The effect of electron cooling due to the dissociation and ionisation costs associated with the reactions of Table 1 is negligible. If the ionisation and dissociation costs (ΔE_{el}) associated with reactions in Table 1 are set to zero, without modifying the reaction rates or kinetic energy release values, the electron temperature and density predicted by SOLPS-ITER at the low-field side strikepoint are within 1% of the reference nitrogen molecular recycling case (Table 2). Although the dissociation cost of the triple bond of the N_2 molecule relates to both the electron cooling and the reaction rate of the dissociation reactions, it is the increase in plasma penetration of nitrogen neutrals and the resulting radiation from nitrogen ions that produces the reduction in electron temperature discussed in Section 5, not the electron cooling due to the dissociation costs.

7. Divertor spectrometer measurements and SOLPS-ITER predictions of line-integrated *N* II, *N* III and *N* IV intensity

When the nitrogen radiated power is fixed to 0.6 MW, SOLPS-ITER predicts that the peak line-integrated emission in the low-field side divertor from *N* II, *N* III and *N* IV in the N_2 molecular recycling simulation is less than the peak intensity in the atomic recycling simulation by approximately 15%, 35% and 5%, respectively (Fig. 6). The predicted density of N^+ ions near the low-field side strike point in the atomic recycling case (Fig. 7) is approximately 3 to 4 times greater than in the molecular recycling case when $P_{rad,N}$ is fixed to 0.6 MW, whereas the predicted densities from the midpoint of the low-field side divertor leg to the X-point are approximately equal. The predicted densities of N^{2+} and N^{3+} in the low-field side divertor volume are approximately within a factor 1.5 in both simulations. The preceding predictions of nitrogen line intensity and ion densities are consistent with the hypothesis that due to the enhanced plasma penetration of neutral nitrogen, nitrogen molecular recycling increases the access of singly-charged nitrogen ions into high-temperature areas of the divertor plasma. The higher fraction of N^+ ions reaching high-temperature areas of the plasma in the molecular recycling case increases the emitted *N* II line radiation per ion and the likelihood of singly-charged nitrogen ions to ionise further relative to atomic recycling of nitrogen.

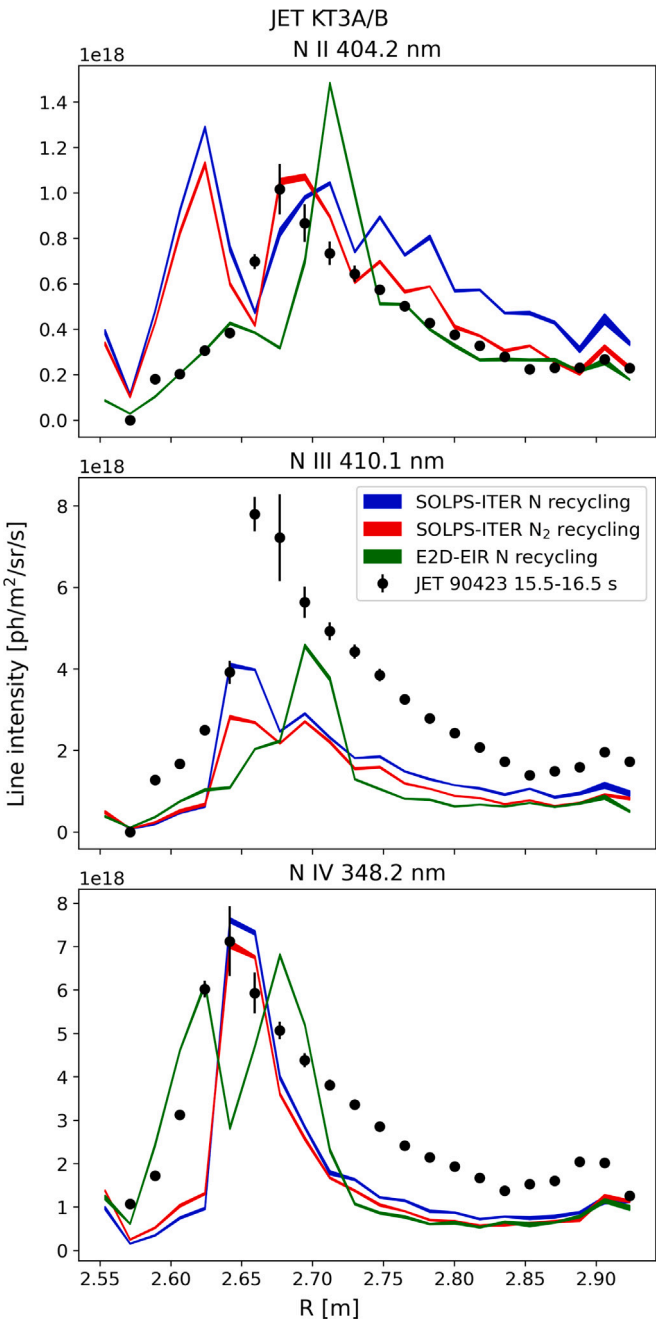

Fig. 6. Line-integrated *N* II, *N* III and *N* IV line intensity in the divertor predicted by SOLPS-ITER under the atomic and molecular recycling assumptions (blue and red lines, respectively), predicted by EDGE2D-EIRENE (green) and measured by the KT3 vertically-viewing mirror-link divertor spectrometer (black dots). The thickness of the solid lines (simulations) indicates the standard deviation associated with repeated post-processing runs using Cherab and the error bars on the dots (KT3 measurements) indicate standard deviation over the time interval $t = 15.5$ s to 16.5 s in the experiment. The nitrogen radiated power is fixed to 0.6 MW in the simulations and the electron density at the low-field side midplane separatrix $n_{e,sep,LFS-mp}$ is fixed to 1.8×10^{19} m^{-3}. (For interpretation of the references to colour in this figure legend, the reader is referred to the web version of this article.)

Under the molecular recycling assumption, the SOLPS-ITER predicted *N* II, *N* III and *N* IV peak intensities are within approximately 15%, 65% and 2% of the measured peak intensity, while under the atomic recycling assumption they are within approximately 30%, 50% and 5% of the measured values, respectively (Fig. 6). The predicted *N* II intensity towards the low-field side in the molecular recycling case is

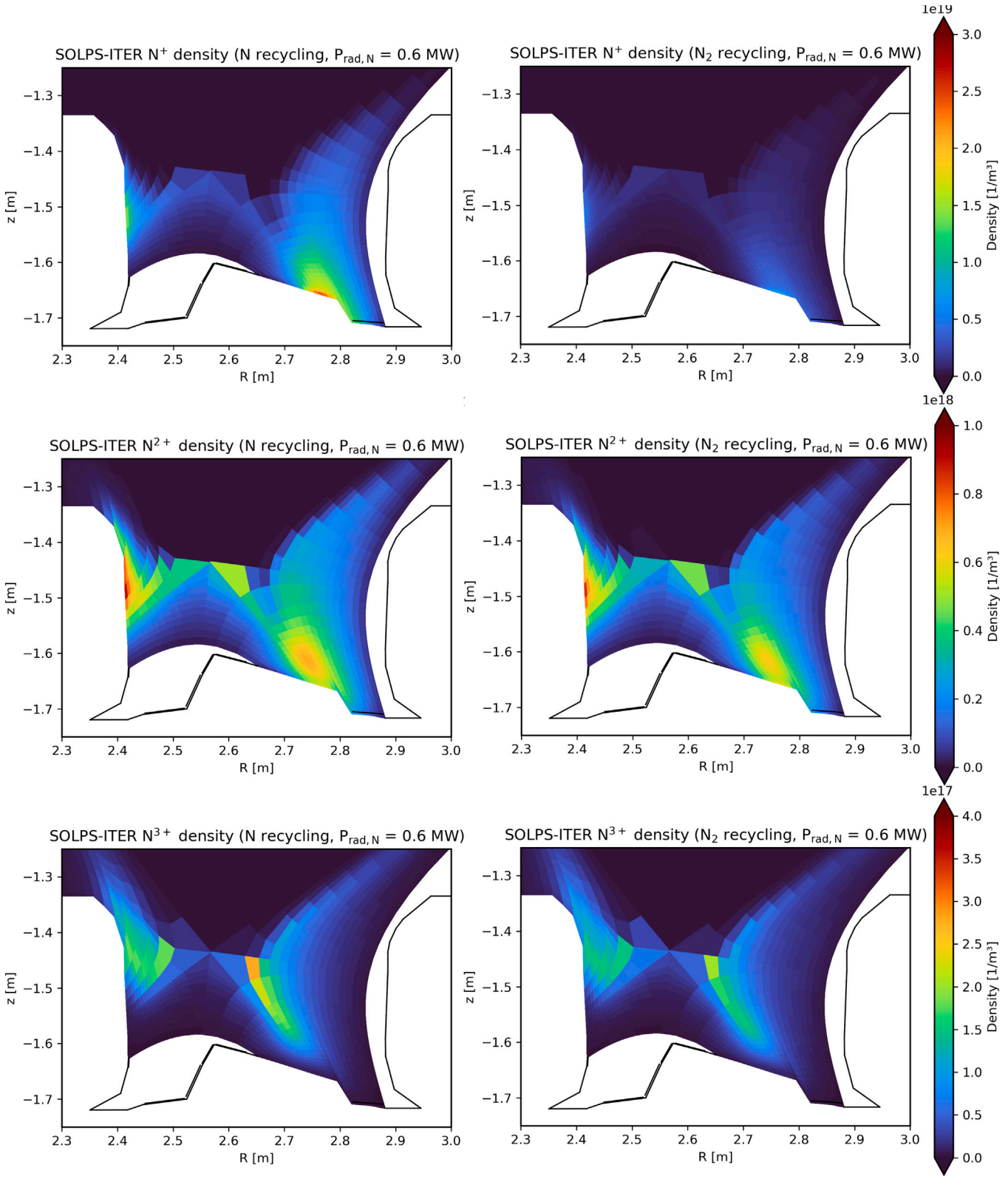

Fig. 7. Density of N^+, N^{2+} and N^{3+} in the divertor predicted by SOLPS-ITER under the atomic and molecular recycling assumptions (left and right columns, respectively). The nitrogen injection rate is set to 20×10^{19} and 6×10^{19} N atoms per second in the atomic and molecular recycling simulations, respectively, yielding a predicted nitrogen radiated power of approximately 0.6 MW in both simulations. The electron density at the low-field side midplane separatrix $n_{e,sep,LFS-mp}$ is fixed to $1.8 \times 10^{19}\,m^{-3}$.

more consistent with the measurements than in the atomic recycling case. However, in both cases, an N II intensity peak is predicted towards the high-field side but is not observed in the experiment. The N III intensity predicted by SOLPS-ITER under the atomic recycling case is more consistent with the measurements than under the molecular recycling assumption, whereas the predictions of peak N IV intensity under

either assumption are within the uncertainty of the measurement. We therefore contend that neither assumptions yields predictions that are overall more consistent with the measurements than the other.

8. EDGE2D-EIRENE and ERo2.0 predictions of line-integrated *N* II, *N* III and *N* IV intensity

In the EDGE2D-EIRENE simulations which assume nitrogen atomic recycling and where the nitrogen radiated power is fixed to 0.6 MW (at a nitrogen injection rate of 6.1×10^{19} *N* atoms per second), the predicted peak intensities are within 45%, 45% and 5% of the measured *N* II, and *N* III and *N* IV peak intensities, respectively (Fig. 6). Assuming nitrogen to recycle as N_2 molecules instead of *N* atoms, ERO2.0 predicts that the peak line-integrated intensity of *N* II, *N* III and *N* IV is increased by 25%, 30% and 20%, respectively, when a constant nitrogen injection rate of 6.1×10^{19} *N* atoms per second is used in both simulations. ERO2.0 simulations conducted on static background plasmas are therefore less sensitive to the nitrogen molecular recycling assumption than the self-consistent SOLPS-ITER simulations where up to a factor of four increase in $P_{\mathrm{rad,N}}$ is predicted under the molecular recycling assumption (Section 5). Compared to the measurements made by the vertically-viewing divertor spectrometer system (KT3), ERO2.0 overestimates the peak line-integrated intensity of *N* II, *N* III and *N* IV by a factor 3.4, 1.05 and 1.5, respectively, when nitrogen is assumed to recycle as atoms, and by a factor 4.1, 1.3 and 1.7, respectively, under the molecular recycling assumption.

The predicted relative increase in the line-integrated *N* III and *N* IV intensity when assuming nitrogen molecular recycling in the ERO2.0 simulations of the current work (30% and 20%, respectively) is smaller than the factor of two increase in peak line-integrated *N* III and *N* IV intensity reported in [7] due to the missing fast reflections of nitrogen ions and atoms in the previous contribution. The impact of fast reflections of nitrogen ions and atoms is qualitatively similar to that of molecular recycling, i.e. the greater kinetic energy of the reflected atoms compared to thermally recycled atoms increases plasma penetration. Thus, the lack of fast reflections of nitrogen ions and atoms in the previous contribution led to an overestimation of the relative impact of nitrogen molecular recycling on static background plasmas and the coincidental improvement of the agreement between the ERO2.0 predictions and measurements of peak line-integrated *N* III and *N* IV intensity.

9. Discussion

In the SOLPS-ITER simulations in which nitrogen recycles as *N* atoms, the steady-state nitrogen injection (and pumping) rate at which the bolometric estimate of 0.6 MW of power radiated by nitrogen is reached is lower than the experimental injection rate by approximately a factor of 7–8. When nitrogen is assumed to recycle as molecules in the SOLPS-ITER simulations, the steady-state injection and pumping rate at which $P_{\mathrm{rad,N}} = 0.6$ MW is reached is lower than the experimental injection rate by approximately a factor of 25–30. Consistently, when nitrogen molecular recycling is assumed, the density of N_2 predicted by SOLPS-ITER in the divertor, including in the volume next to the low-field side pumping plenum, is approximately one fifth of the *N* density when atomic recycling is assumed (in the case of molecular recycling, the nitrogen neutral density is dominated by N_2). Thus, in the SOLPS-ITER molecular recycling simulation, less nitrogen is injected, the density of neutral nitrogen species is lower and less nitrogen is being pumped than in the atomic recycling simulation. EDGE2D-EIRENE simulations (where nitrogen recycles as atoms) predict a steady-state injection and pumping rate at which $P_{\mathrm{rad,N}} = 0.6$ MW that is approximately a factor of three lower than in the SOLPS-ITER nitrogen atomic recycling simulations, possibly due to the remaining differences in the boundary conditions or a yet unidentified numerical issue present in one code but not the other.

The discrepancy between the nitrogen injection in the experiment and in the codes may stem from (1) missing physics in the simulations, such as non-resonant charge-exchange reactions between main ions and the nitrogen impurities, (2) numerical issues such as insufficient spatial resolution of the grids near the X-point, (3) the quadrangular, magnetically-aligned grids of the plasma fluid codes not extending all the way to the vertical surface of the low-field side divertor, (4) an overestimation of the albedo of the low-field side pumping surface (here, 0.8) for nitrogenic species, (5) the omission of the subdivertor volume and the cryopump therein, (6) a plasma solution that is not representative of the experimental divertor conditions, (7) direct pumping of injected nitrogen gas, (8) incomplete saturation of the JET plasma-facing components in the experiment or (9) the formation of ammonia molecules and their subsequent sticking to plasma-shadowed areas. To address items 1, 2, 3, 4 and 5, the missing ion-neutral reactions should be included in the model, the grid resolution increased, the wide-grid version [17] of the SOLPS-ITER code employed, the effective albedo of the low-field side pumping surface determined for nitrogenic species as in [13] for hydrogenic species and the impact of including the subdivertor volume investigated, respectively. Items 6, 7, 8 and 9 are discussed below.

SOLPS-ITER and EDGE2D-EIRENE underestimate the line-integrated electron temperature and peak electron density towards the low-field side from the strike point by approximately a factor of two when the power radiated by nitrogen is set to 0.6 MW, independent of whether nitrogen is assumed to recycle as atoms or molecules in the SOLPS-ITER simulations (Fig. 8). The difficulty in matching the predicted and measured plasma conditions in high-density, low-confinement mode JET divertor plasmas using SOLPS-ITER and EDGE2D-EIRENE is not limited to nitrogen-seeded discharges, see e.g. [18]. Line emission due to electron impact excitation is linearly proportional to the electron density and the photon emissivity coefficient, which itself is sensitive to electron temperature and density. Furthermore, electron density and temperature affect nitrogen transport and hence nitrogen emission by modifying, for instance, the ionisation rate and the temperature gradient force acting on nitrogen ions, respectively.

In nitrogen-seeded ASDEX Upgrade discharges, up to 90% of the seeded N_2 gas was found to "bypass" the plasma, i.e. not dissociate or ionise, but instead enter the pumping ducts directly [22]. The simulations in this work are unlikely to capture such a bypass effect, since the injected neutral nitrogen atoms move along straight trajectories until they impact a wall, become ionised or are pumped, with pumping being less likely than ionisation due to geometric reasons and the non-zero albedo of the pumping surface. The lack of a bypass mechanism in the simulations allowing up to 90% of the injected nitrogen to be pumped directly is thus a possible cause of the discrepancy between the steady-state injection and pumping rates in the simulations and the experiment.

In this contribution, we have assumed all of the plasma-facing components of the JET ITER-like wall to be saturated with nitrogen in the experiment (and consistently assumed nitrogen to be a fully-recycling species in the simulations) as the JET pulses 90422 and 90423 were preceded by five nitrogen-seeded discharges. In ASDEX Upgrade, three subsequent nitrogen-seeded discharges were sufficient to saturate the all-tungsten plasma-facing components via nitrogen ion implantation [23], whereas in JET a larger number of discharges may be needed due to the possibility of co-deposition of nitrogen with beryllium [24]. Deuterated ammonia has been detected in the exhaust gases of ASDEX Upgrade and JET [24]. Its formation and retention in the plasma-shadowed areas of the vessel, which is not accounted for in the simulations, is another mechanism which may contribute to the higher steady-state injection and pumping rates in the experiment compared to the simulations.

Building a computational ammonia formation, transport and dissociation model is the subject of a future publication. Nitrogen recycling in part as ammonia molecules is expected to increase the plasma

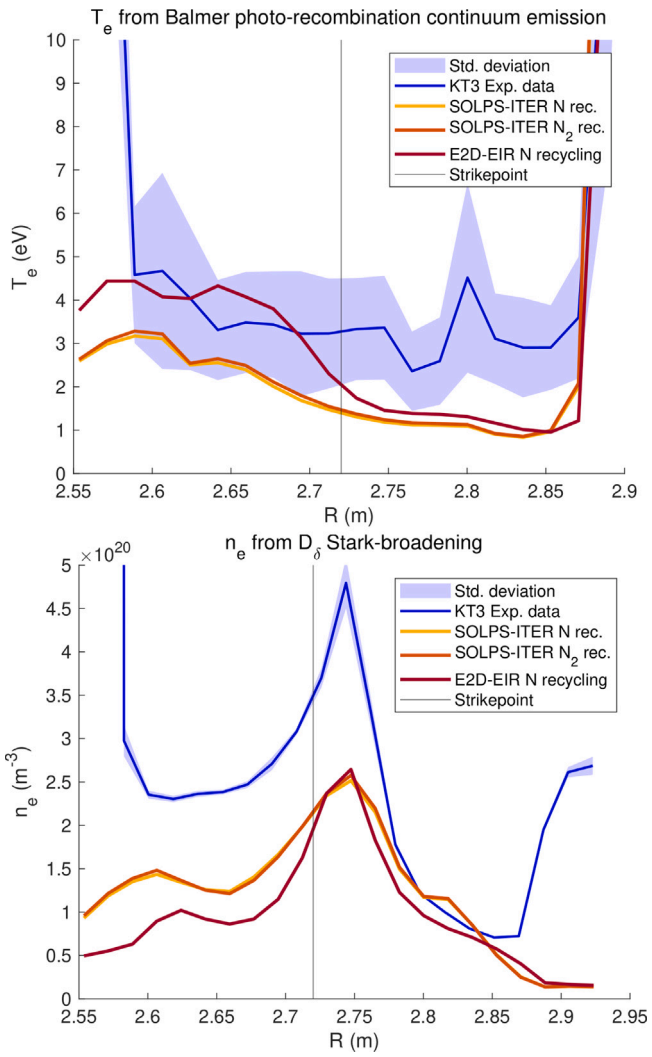

Fig. 8. Line-integrated electron temperature and electron density (blue lines) inferred from Balmer photo-recombination continuum emission [19] and D_δ Stark-broadening [20], respectively, and the corresponding predictions from EDGE2D-EIRENE (red) and SOLPS-ITER under the nitrogen atomic and molecular recycling assumptions (yellow and orange) post-processed using the PESDT code (formerly, pyproc) [21]. The blue shaded area indicates the standard deviation over the time interval t = 15.5 s to 16.5 s in the experiment. The nitrogen radiated power is fixed to 0.6 MW in the simulations and the electron density at the low-field side midplane separatrix $n_{e,sep,LFS-mp}$ is fixed to $1.8 \times 10^{19}\,m^{-3}$. (For interpretation of the references to colour in this figure legend, the reader is referred to the web version of this article.)

penetration of neutral nitrogen species similar to recycling as N_2, as kinetic energy release values of the same order as in Table 1 have been measured in e.g. the dissociative excitation of NH^+ [25]. However, due to the disparity in mass between nitrogen and deuterium, a smaller fraction of the released kinetic energy is imparted onto the nitrogen-containing dissociation fragment in the dissociation reactions of e.g. ND_3, ND_2 and ND than in the dissociation of N_2.

10. Conclusions

Assuming nitrogen to recycle as N_2 molecules instead of N atoms in SOLPS-ITER simulations of nitrogen-seeded, partially detached JET L-mode plasmas increases the power radiated by nitrogen ions by up to a factor of four and reduces the electron temperature locally in the low-field side divertor leg by up to an order of magnitude when a fixed nitrogen injection rate is used. The increase in nitrogen radiated power occurs due to an increase in the abundance of nitrogen ions by 80% (for N^+) to 600% (for N^{2+}). Enhanced plasma penetration of nitrogen atoms due to the high dissociation threshold of triply-bonded N_2 molecules and the kinetic energy release in the dissociation event is shown to explain the increase in the nitrogen ion abundance.

When the power radiated by nitrogen ions is matched to the bolometric estimate from experiment by adjusting the nitrogen injection rate, the SOLPS-ITER N_2 recycling simulations predict peak line-integrated N II to N IV intensities within 5% to 35% of the atomic recycling case, and both simulations predict peak line-integrated N II to N IV intensities within 5% to 65% of the values measured by the vertically-viewing divertor spectrometer. Neither recycling assumption yields predictions that are overall more consistent with the measurements of line-integrated N II to N IV intensity than the other when the nitrogen injection rate is treated as a free parameter. If a fixed nitrogen injection rate is used in e.g. predictive modelling, a sensitivity analysis testing both atomic and molecular nitrogen recycling is recommended. However, the discrepancy between the steady-state nitrogen injection rates in the simulations and experiments described in Section 9 must be resolved before predictive modelling with fixed nitrogen injection rates is possible.

CRediT authorship contribution statement

R. Mäenpää: Writing – original draft, Visualization, Methodology, Investigation, Conceptualization. **H. Kumpulainen:** Software, Conceptualization. **M. Groth:** Writing – review & editing, Supervision, Project administration, Funding acquisition, Data curation, Conceptualization. **N. Horsten:** Writing – review & editing, Software, Methodology, Conceptualization. **D. Reiter:** Writing – review & editing, Software, Methodology, Data curation, Conceptualization. **J. Romazanov:** Software, Conceptualization. **B. Lomanowski:** Software, Methodology, Data curation, Conceptualization. **S. Brezinsek:** Supervision, Conceptualization. **J. Karhunen:** Writing – review & editing, Software, Data curation, Conceptualization. **K.D. Lawson:** Investigation, Data curation. **A.G. Meigs:** Investigation, Data curation. **S. Menmuir:** Investigation, Data curation. **A. Shaw:** Investigation, Data curation.

Declaration of competing interest

The authors declare that they have no known competing financial interests or personal relationships that could have appeared to influence the work reported in this paper.

Acknowledgements

This work has been carried out within the framework of the EUROfusion Consortium, funded by the European Union via the Euratom Research and Training Programme (Grant Agreement No 101052200 — EUROfusion). Views and opinions expressed are however those of the author(s) only and do not necessarily reflect those of the European Union or the European Commission. Neither the European Union nor the European Commission can be held responsible for them. This work made use of the Triton cluster, part of the Science-IT project at Aalto University. N. Horsten is a postdoctoral fellow of the Research Foundation Flanders (FWO) under grant number 12AES24N. We gratefully acknowledge the invaluable code support provided by Dr. Xavier Bonnin and Dr. David Coster.

Appendix A. Catalogue of simulations

See Table A.3

Data availability

The authors do not have permission to share data.

Table A.3
SOLPS-ITER simulations are stored on the MPCDF TOK cluster under "/toks/work/rmaenpaa/solps-iter/runs/jet/81472/", the ERO2.0 simulations are stored on the Aalto Triton cluster under "/scratch/phys/fusion/ero/runs/rmaenpaa/jet/" and the EDGE2D-EIRENE simulations are stored on the JET Data Centre cluster under "/home/rmaenpaa/cmg/catalog/edge2d/jet/81472/".

Code	Directory	Description
SOLPS-ITER	case89	N only
	case90	N_2 rec.
	case92	N_2 rec., KER/10^3
	case93	N_2 rec., KER/10^3, $\langle\sigma v\rangle_{2.7.5} \cdot 50$
	case124	N_2 rec., $\Delta E_{el} = 0\,eV$
ERO2.0	run183/seq01	N only
	run186/seq01	N_2 rec.
EDGE2D-EIRENE	mar2123/seq#1	N only

References

[1] A. Huber, M. Wischmeier, M. Bernert, S. Wiesen, S. Glöggler, S. Aleiferis, S. Brezinsek, G. Calabro, P. Carvalho, V. Huber, G. Sergienko, E.R. Solano, C. Giroud, M. Groth, S. Jachmich, C. Linsmeier, G.F. Matthews, A.G. Meigs, P. Mertens, M. Sertoli, S. Silburn, G. Telesca, JET contributors, Peculiarity of highly radiating multi-impurity seeded H -mode plasmas on JET with ITER-like wall, Phys. Scr. T171 (2020) 014055, http://dx.doi.org/10.1088/1402-4896/ab5753, URL https://iopscience.iop.org/article/10.1088/1402-4896/ab5753.

[2] M. Bernert, F. Janky, B. Sieglin, A. Kallenbach, B. Lipschultz, F. Reimold, M. Wischmeier, M. Cavedon, P. David, M. Dunne, M. Griener, O. Kudlacek, R. McDermott, W. Treutterer, E. Wolfrum, D. Brida, O. Février, S. Henderson, M. Komm, X-point radiation, its control and an ELM suppressed radiating regime at the ASDEX Upgrade tokamak, Nucl. Fusion 61 (2) (2021) 024001, http://dx.doi.org/10.1088/1741-4326/abc936, URL https://iopscience.iop.org/article/10.1088/1741-4326/abc936.

[3] S. Wiesen, D. Reiter, V. Kotov, M. Baelmans, W. Dekeyser, A. Kukushkin, S. Lisgo, R. Pitts, V. Rozhansky, G. Saibene, I. Veselova, S. Voskoboynikov, The new SOLPS-ITER code package, J. Nucl. Mater. 463 (2015) 480–484, http://dx.doi.org/10.1016/j.jnucmat.2014.10.012, URL https://linkinghub.elsevier.com/retrieve/pii/S0022311514006965.

[4] J. Romazanov, D. Borodin, A. Kirschner, S. Brezinsek, S. Silburn, A. Huber, V. Huber, H. Bufferand, M. Firdaouss, D. Brömmel, B. Steinbusch, P. Gibbon, A. Lasa, I. Borodkina, A. Eksaeva, C. Linsmeier, JET Contributors, First ERO2.0 modeling of Be erosion and non-local transport in JET ITER-like wall, Phys. Scr. T170 (2017) 014018, http://dx.doi.org/10.1088/1402-4896/aa89ca, URL https://iopscience.iop.org/article/10.1088/1402-4896/aa89ca.

[5] R. Simonini, G. Corrigan, G. Radford, J. Spence, A. Taroni, Models and numerics in the multi-fluid 2-D edge plasma code EDGE2D/U, Contrib. To Plasma Phys. 34 (2–3) (1994) 368–373, http://dx.doi.org/10.1002/ctpp.2150340242, URL https://onlinelibrary.wiley.com/doi/10.1002/ctpp.2150340242.

[6] D. Reiter, M. Baelmans, P. Börner, The EIRENE and B2-EIRENE codes, Fusion Sci. Technol. 47 (2) (2005) 172–186, http://dx.doi.org/10.13182/FST47-172, URL https://www.tandfonline.com/doi/full/10.13182/FST47-172.

[7] R. Mäenpää, H. Kumpulainen, M. Groth, J. Romazanov, B. Lomanowski, S. Brezinsek, S. Di Genova, J. Karhunen, K. Lawson, A.G. Meigs, S. Menmuir, A. Shaw, EDGE2D-EIRENE and ERO2.0 predictions of nitrogen molecular break-up and transport in the divertor of JET low-confinement mode plasmas, Nucl. Mater. Energy 33 (2022) 101273, http://dx.doi.org/10.1016/j.nme.2022.101273, URL https://www.sciencedirect.com/science/article/pii/S2352179122001545.

[8] A. Meigs, M. Stamp, R. Igreja, S. Sanders, P. Heesterman, JET-EFDA Contributors, Enhancement of JET's mirror-link near-ultraviolet to near-infrared divertor spectroscopy system, Rev. Sci. Instrum. 81 (10) (2010) 10E532, http://dx.doi.org/10.1063/1.3502322, URL https://pubs.aip.org/rsi/article/81/10/10E532/351331/Enhancement-of-JET-s-mirror-link-near-ultraviolet.

[9] B. Lomanowski, M. Carr, A. Field, M. Groth, A. Jaervinen, C. Lowry, A. Meigs, S. Menmuir, M. O'Mullane, M. Reinke, C. Stavrou, S. Wiesen, Spectroscopic investigation of n and Ne seeded induced detachment in JET ITER-like wall L-modes combining experiment and EDGE2D modeling, Nucl. Mater. Energy 20 (2019) 100676, http://dx.doi.org/10.1016/j.nme.2019.100676, URL https://linkinghub.elsevier.com/retrieve/pii/S2352179118302217.

[10] M. Reinke, A. Meigs, E. Delabie, R. Mumgaard, F. Reimold, S. Potzel, M. Bernert, D. Brunner, J. Canik, M. Cavedon, I. Coffey, E. Edlund, J. Harrison, B. LaBombard, K. Lawson, B. Lomanowski, J. Lore, M. Stamp, J. Terry, E. Viezzer, Expanding the role of impurity spectroscopy for investigating the physics of high-z dissipative divertors, Nucl. Mater. Energy 12 (2017) 91–99, http://dx.doi.org/10.1016/j.nme.2016.12.003, URL https://linkinghub.elsevier.com/retrieve/pii/S2352179116302034.

[11] L. Lao, H. St. John, R. Stambaugh, A. Kellman, W. Pfeiffer, Reconstruction of current profile parameters and plasma shapes in tokamaks, Nucl. Fusion 25 (11) (1985) 1611–1622, http://dx.doi.org/10.1088/0029-5515/25/11/007, URL https://iopscience.iop.org/article/10.1088/0029-5515/25/11/007.

[12] W. Eckstein, D. Heifetz, Data sets for hydrogen reflection and their use in neutral transport calculations, J. Nucl. Mater. 145–147 (1987) 332–338, http://dx.doi.org/10.1016/0022-3115(87)90355-2, URL https://linkinghub.elsevier.com/retrieve/pii/0022311587903552.

[13] V. Solokha, M. Groth, S. Brezinsek, M. Brix, G. Corrigan, C. Guillemaut, D. Harting, S. Jachmich, U. Kruezi, S. Marsen, S. Wiesen, The role of drifts on the isotope effect on divertor plasma detachment in JET Ohmic discharges, Nucl. Mater. Energy 25 (2020) 100836, http://dx.doi.org/10.1016/j.nme.2020.100836, URL https://linkinghub.elsevier.com/retrieve/pii/S235217912030106X.

[14] M. Groth, V. Solokha, S. Aleiferis, S. Brezinsek, M. Brix, I. Carvalho, P. Carvalho, G. Corrigan, D. Harting, N. Horsten, I. Jepu, J. Karhunen, K. Kirov, B. Lomanowski, K. Lawson, C. Lowry, A. Meigs, S. Menmuir, E. Pawelec, T. Pereira, A. Shaw, S. Silburn, B. Thomas, S. Wiesen, P. Börner, D. Borodin, S. Jachmich, D. Reiter, G. Sergienko, Z. Stancar, B. Viola, P. Beaumont, J. Bernardo, I. Coffey, N. Conway, E. De La Luna, D. Douai, C. Giroud, J. Hillesheim, L. Horvath, A. Huber, P. Lomas, C. Maggi, M. Maslov, C. Perez Von Thun, S. Scully, N. Vianello, M. Wischmeier, Characterisation of divertor detachment onset in JET-ILW hydrogen, deuterium, tritium and deuterium–tritium low-confinement mode plasmas, Nucl. Mater. Energy 34 (2023) 101345, http://dx.doi.org/10.1016/j.nme.2022.101345, URL https://linkinghub.elsevier.com/retrieve/pii/S2352179122002265.

[15] D. Reiter, The data file AMJUEL: Additional atomic and molecular data for EIRENE, Forschungszentrum Juelich GmbH 52425 (2000).

[16] M. Carr, A. Meakins, M. Bernert, P. David, C. Giroud, J. Harrison, S. Henderson, B. Lipschultz, F. Reimold, EUROfusion MST1 Team, ASDEX Upgrade Team, Description of complex viewing geometries of fusion tomography diagnostics by ray-tracing, Rev. Sci. Instrum. 89 (8) (2018) 083506, http://dx.doi.org/10.1063/1.5031087, URL https://pubs.aip.org/rsi/article/89/8/083506/990546/Description-of-complex-viewing-geometries-of.

[17] W. Dekeyser, P. Boerner, S. Voskoboynikov, V. Rozhanksy, I. Senichenkov, L. Kaveeva, I. Veselova, E. Vekshina, X. Bonnin, R. Pitts, M. Baelmans, Plasma edge simulations including realistic wall geometry with SOLPS-ITER, Nucl. Mater. Energy 27 (2021) 100999, http://dx.doi.org/10.1016/j.nme.2021.100999, URL https://linkinghub.elsevier.com/retrieve/pii/S2352179121000788.

[18] N. Horsten, M. Groth, V.-P. Rikala, B. Lomanowski, A. Meigs, S. Aleiferis, X. Bonnin, G. Corrigan, W. Dekeyser, R. Futtersack, D. Harting, D. Reiter, V. Solokha, B. Thomas, S. Van Den Kerkhof, N. Vervloesem, Validation of SOLPS-ITER and EDGE2D-EIRENE simulations for H, D, and T JET ITER-like wall low-confinement mode plasmas, Nucl. Mater. Energy 42 (2025) 101842, http://dx.doi.org/10.1016/j.nme.2024.101842, URL https://linkinghub.elsevier.com/retrieve/pii/S2352179124002655.

[19] B. Lomanowski, A. Meigs, R. Sharples, M. Stamp, C. Guillemaut, Inferring divertor plasma properties from hydrogen Balmer and Paschen series spectroscopy in JET-ILW, Nucl. Fusion 55 (12) (2015) 123028, http://dx.doi.org/10.1088/0029-5515/55/12/123028, URL https://iopscience.iop.org/article/10.1088/0029-5515/55/12/123028.

[20] A. Meigs, S. Brezinsek, M. Clever, A. Huber, S. Marsen, C. Nicholas, M. Stamp, K.-D. Zastrow, Deuterium Balmer/Stark spectroscopy and impurity profiles: First results from mirror-link divertor spectroscopy system on the JET ITER-like wall, J. Nucl. Mater. 438 (2013) S607–S611, http://dx.doi.org/10.1016/j.jnucmat.2013.01.127, URL https://linkinghub.elsevier.com/retrieve/pii/S0022311513001359.

[21] B. Lomanowski, Plasma emission synthetic diagnostic toolkit, 2024, URL https://github.com/lomanowski/PESDT.

[22] T. Reichbauer, A. Drenik, R. McDermott, V. Rohde, Assessment of nitrogen fluence from the divertor plasma in nitrogen seeded discharges, Fusion Eng. Des. 149 (2019) 111325, http://dx.doi.org/10.1016/j.fusengdes.2019.111325, URL https://linkinghub.elsevier.com/retrieve/pii/S092037961930821X.

[23] M. Oberkofler, D. Alegre, F. Aumayr, S. Brezinsek, T. Dittmar, K. Dobes, D. Douai, A. Drenik, M. Köppen, U. Kruezi, C. Linsmeier, C. Lungu, G. Meisl, M. Mozetic, C. Porosnicu, V. Rohde, S. Romanelli, Plasma–wall interactions with nitrogen seeding in all-metal fusion devices: Formation of nitrides and ammonia, Fusion Eng. Des. 98–99 (2015) 1371–1374, http://dx.doi.org/10.1016/j.fusengdes.2015.01.044, URL https://linkinghub.elsevier.com/retrieve/pii/S092037961500071X.

[24] M. Oberkofler, G. Meisl, A. Hakola, A. Drenik, D. Alegre, S. Brezinsek, R. Craven, T. Dittmar, T. Keenan, S.G. Romanelli, R. Smith, D. Douai, A. Herrmann, K. Krieger, U. Kruezi, G. Liang, C. Linsmeier, M. Mozetic, V. Rohde, the ASDEX Upgrade team, the EUROfusion MST1 Team, JET Contributors, Nitrogen retention mechanisms in tokamaks with beryllium and tungsten plasma-facing surfaces, Phys. Scr. T167 (2016) 014077, http://dx.doi.org/10.1088/0031-8949/T167/1/014077, URL https://iopscience.iop.org/article/10.1088/0031-8949/T167/1/014077.

[25] J. Lecointre, D.S. Belic, S. Cherkani-Hassani, P. Defrance, Electron impact dissociation of ND+: formation of D+, Eur. Phys. J. D 63 (3) (2011) 441–448, http://dx.doi.org/10.1140/epjd/e2011-20221-2, URL http://link.springer.com/10.1140/epjd/e2011-20221-2.